Atmospheric turbidity forecasting using side-by-side ANFIS

Julien Nou, Rémi Chauvin, Adama Traoré, Stéphane Thil, Stéphane Grieu

Available online at www.sciencedirect.com

ScienceDirect

Energy Procedia 49 (2014) 2387 – 2397

Energy Procedia

SolarPACES 2013

Atmospheric turbidity forecasting using side-by-side ANFIS

J. Nou[1,*], R. Chauvin[1,2], A. Traoré[1,2], S. Thil[1,2] and S. Grieu[1,2]

[1]*PROMES-CNRS, Rambla de la thermodynamique, Tecnosud, 66100 Perpignan, France*
[2]*University of Perpignan Via Domitia, 52 Avenue Paul Alduy, 66860 Perpignan, France*

Abstract

In a context of sustainable development, enthusiasm for CSP technologies is increasing. In addition, the CSPIMP (Concentrated Solar Power efficiency IMProvement) European project has been recently initiated to achieve a better competitiveness of the CSP plants. Its main objective is to develop a new procedure to improve the steam turbine start up cycles, maintenance activities and advanced plant control schemes. A challenge in the project is to forecast the solar resource with the aim of improving the management of CSP plants. A key parameter when trying to estimate or forecast solar radiation is atmospheric turbidity. Indeed, the Direct Normal Irradiance (DNI) under clear sky conditions can be expressed as a function of extraterrestrial irradiation, altitude and atmospheric turbidity. So, this paper focuses on forecasting atmospheric turbidity at different time horizons (up to 3 hours) using side-by-side Adaptive Network-based Fuzzy Inference Systems (ANFIS). First, a Multi-Resolution Analysis (MRA) based on the discrete wavelet transform allowed clear sky DNI values to be extracted from the NREL database. In addition, a Principal Component Analysis (PCA) has been considered in order to develop the forecasting model using uncorrelated input variables and reduce its complexity (and, as a consequence, computation time). Finally, the results we obtained about atmospheric turbidity forecasting are satisfactory and validate the proposed approach.

Selection and peer review by the scientific conference committee of SolarPACES 2013 under responsibility of PSE AG.
Final manuscript published as received without editorial corrections.

Keywords: Atmospheric turbidity forecasting, adaptive network-based fuzzy inference system, principal component analysis, wavelet-based multi-resolution analysis.

1. Introduction

Having an accurate knowledge about Direct Normal Irradiance (DNI) is of high interest in many solar energy applications like Concentrated Solar Power (CSP). As part of the CSPIMP (Concentrated Solar Power efficiency

* Corresponding author. Tel.: +33468682706; fax: +33468682213.
E-mail address: julien.nou@promes.cnrs.fr

Selection and peer review by the scientific conference committee of SolarPACES 2013 under responsibility of PSE AG.
Final manuscript published as received without editorial corrections.
doi:10.1016/j.egypro.2014.03.253

IMProvement) European project, which focuses on optimizing the performance of CSP plants, the present work is related to solar resource forecasting. The project began in may 2012 and includes the PROMES-CNRS laboratory and three industrial partners: ACCIONA Energía (one of the world leaders in the renewable sector), Thermodyn (which is specialized in the supply of turbomachinery and services for the oil and gas industry) and Nuovo Pignone (an industry's supplier of turbo-machinery, compressors, pumps, static equipment and metering systems). A challenge in the CSPIMP project is to develop an effective predictive model about solar resource (DNI). In order to improve the management of CSP plants, short-term (5-30 minutes) and medium-term (a few hours) forecasting procedures are well adapted to large fluctuations in solar radiation. Moreover, changes in the DNI are mainly attributable to two factors: the presence of clouds and atmospheric turbidity. Before reaching the surface of the Earth, the extraterrestrial solar radiation is attenuated in its passage through the atmosphere and can also be reduced in case of clouds.

Many works have already been realized about DNI forecasting with short-term or medium-term horizons. Among all of these works, one can highlight the two studies realized by Marquez and Coimbra. In the first one [1], the authors developed a medium-term solar irradiance forecasting model based on Artificial Neural Networks (ANN). Marquez and Coimbra adopted predicted meteorological variables from the US National Weather Service's (NWS) forecasting database as inputs to the proposed model without taking into account the cloud detection (by ground-based camera images or satellite images). The second study [2] is about the development of an image processing methodology (images are provided by a Total Sky Imager (TSI)) to forecast the DNI at short-term horizon and at the ground level. The authors focused on forecasting 1-min averaged DNI values for various time horizons (from 3 to 15 minutes). As a negative point, the DNI under clear sky conditions was supposed to be constant during the considered period of time. As a consequence, to obtain a good accuracy when forecasting DNI, we propose a new methodology based on efficient models about cloud cover estimation and atmospheric turbidity forecasting. So, the present paper deals with a methodology to forecast atmospheric turbidity at different time horizons. As a key point, we used data provided by the NREL (National Renewable Energy Laboratory, Golden, Colorado, USA). In addition, complex changes in atmospheric turbidity as well as abundant historical data suggest that artificial intelligence techniques are good candidates to forecast atmospheric turbidity accurately from meteorological variables. As a result, side-by-side Adaptive Network-based Fuzzy Inference Systems (ANFIS) are used. In the field of artificial intelligence, neural networks and fuzzy logic can be combined in neuro-fuzzy systems in order to achieve both properties of readability and learning ability. Neuro-fuzzy systems synergizes the two techniques by combining the human-like reasoning style of fuzzy systems (through the use of fuzzy sets and a linguistic model consisting of a set of if-then fuzzy rules) with the learning and connectionist structure of artificial neural networks [3,4].

First, a Multi-Resolution Analysis (MRA) based on the discrete wavelet transform allowed DNI values under clear sky conditions (clear sky DNI) to be extracted from the NREL database. We generated historical data about atmospheric turbidity (T_{LI}) using the empirical formulation proposed by Ineichen and Perez. In addition, a Principal Component Analysis (PCA) has been considered in order to develop the forecasting model using uncorrelated input variables. PCA is a useful statistical technique based on orthogonal transformation allowing a set of correlated variables to be converted into a new set of linearly uncorrelated variables called principal components. As it is well known in the field of artificial intelligence, highly correlated input variables impact on learning ability in a negative way. Moreover, PCA allows both the complexity of the developed model and computation time to be significantly reduced. The considered side-by-side ANFIS allow atmospheric turbidity to be forecasted at different time horizons ranging from 1 hour to 3 hours.

The paper is organized as follows: section 2 is about atmospheric turbidity considerations. Section 3 focuses on the materials and methods. All the tools used as well as the proposed forecasting approach are described in this section. Section 4 deals with the results about atmospheric turbidity forecasting we obtained. The paper ends with a conclusion and outlook on further work.

2. Considerations about atmospheric turbidity

The atmosphere is composed of two aerosol particles categories disposed in two dominant layers. The first layer, located at 0-3 km of the Earth's surface, is affected by natural phenomena and anthropogenic activities. The second one, called stratospheric dust layer and located at 15-25 km, results from volcanic activities and cosmic rays [5]. The Linke turbidity coefficient T_L [6] is the first formulation proposed for atmospheric turbidity. Such a formulation is

based on the number of clean dry atmospheres leading to the observed attenuation of solar radiation. For example, in Europe, during summer, the water vapor is often large and the blue sky is close to white: T_L is larger than 3. In opposition, in turbid atmosphere (in polluted cities), T_L is close to 6 or 7. This formulation was widely used since 1922, because of an easy implementation. However, it is dependent on air mass [7,8,9]. That is why, in 2002, Ineichen and Perez proposed a new formulation of the Linke turbidity coefficient in order to avoid its dependence upon solar geometry. They developed a simple clear sky model for direct normal irradiance [10]. Introducing the Linke turbidity coefficient at air mass 2 (T_{LK}) and a multiplicative coefficient b taking into account the altitude of the considered site A_S, Ineichen and Perez obtained an empirical formulation of the normal clear sky radiation I_{bn} (1,2):

$$I_{bn} = bI_0.exp\left(-0.09.AM.(T_{LK} - 1)\right) \quad (1)$$

$$b = 0.664 + \frac{0.163}{exp\left(\frac{-A_S}{8000}\right)} \quad (2)$$

I_0 is the extraterrestrial irradiance at normal incidence and AM the altitude-corrected air mass [9]. From equation (1), one can obtain T_{LI} easily when the normal clear sky radiation I_{bn} and the geographical characteristics of a given site (latitude, longitude and altitude) are known (3):

$$T_{LI} = 1 + \left[\frac{11.1}{AM} \cdot \ln\left(\frac{bI_0}{I_{bn}}\right)\right] \quad (3)$$

3. Materials and methods

3.1. NREL database

The database we used to develop and validate the proposed atmospheric turbidity model is composed of data collected by the NREL (National Renewable Energy Laboratory) in Golden, Colorado, USA (latitude is 39.74° N, longitude is 105.18° W and elevation is 1829 m). Data can be downloaded at http://midcdmz.nrel.gov/apps. An exhaustive set of meteorological parameters and irradiances is available, data being collected since July 1981. We considered the following variables to forecast atmospheric turbidity: Direct Normal Irradiance (DNI), Dry-Bulb Temperature (DBT), Relative Humidity (RH), and Pressure (P). We selected measurements from 2002 to 2013 with a time step of one minute.

3.2. Overall approach

The study we present in this paper is subdivided into three main parts (Fig. 1). The first one is a preliminary analysis (Fig. 1.a) of the selected measurements from the NREL database. What is needed to develop and validate the forecasting model about atmospheric turbidity (Fig. 1.c) is first DNI under clear sky conditions (clear sky DNI). As a result, we needed a procedure allowing clear sky data to be extracted from the database and we decided for a wavelet-based multi-resolution analysis. With such an analysis, based on the Discrete Wavelet Transform (DWT), one can detect the presence of clouds in the sky. Basically, a wavelet-based multi-resolution analysis allows a given signal to be decomposed into approximations (i.e. low-frequency coefficients) and details (i.e. high-frequency coefficients) thanks to a filter bank composed of Low-Pass (LP) and High-Pass (HP) filters. As a result, significant changes in the DNI, related to the presence of clouds in the sky, can be highlighted in the detail coefficients. We used equation (3) to obtain historical data about T_{LI} from clear sky DNI values. The second part of the work (Fig. 1.b) is related to the search for the best input model variables. As it is well known, highly correlated variables impact on learning ability in a negative way. As a consequence, a Principal Component Analysis (PCA) has been considered in order to generate a set of linearly uncorrelated (synthetic) variables from the set of NREL (possibly correlated) variables. So, PCA has been applied to the following variables: Day (D), Hour (H), Dry-Bulb Temperature (DBT), Pressure (Pu), and Relative Humidity (RH). Finally, the third and main part of the work is about the development

and validation of the atmospheric turbidity forecasting model (Fig. 1.c). The proposed model consists in four blocs (i.e. four side-by-side ANFIS) with each bloc giving current ($T_{LI}(t)$) and future ($T_{LI}(t+1h)$, $T_{LI}(t+2h)$ and $T_{LI}(t+3h)$) values of atmospheric turbidity. As previously mentioned in the paper, complex changes in atmospheric turbidity as well as abundant historical data available suggest that artificial intelligence techniques are good candidates to forecast atmospheric turbidity accurately. As a result, four side-by-side Adaptive Network-based Fuzzy Inference Systems (ANFIS) are used. In the field of artificial intelligence, neural networks and fuzzy logic can be combined in neuro-fuzzy systems in order to achieve both properties of readability and learning ability. Neuro-fuzzy systems synergizes the two techniques by combining the human-like reasoning style of fuzzy systems (through the use of fuzzy sets and a linguistic model consisting of a set of if-then fuzzy rules) with the learning and connectionist structure of artificial neural networks [3, 4]. Finally, we generated 84000 examples to train (56000) and validate (28000) the side-by-side ANFIS, considering an inputs/output time interval of 1 hour (bloc 1), 2 hours (bloc 2) and 3 hours (bloc 3).

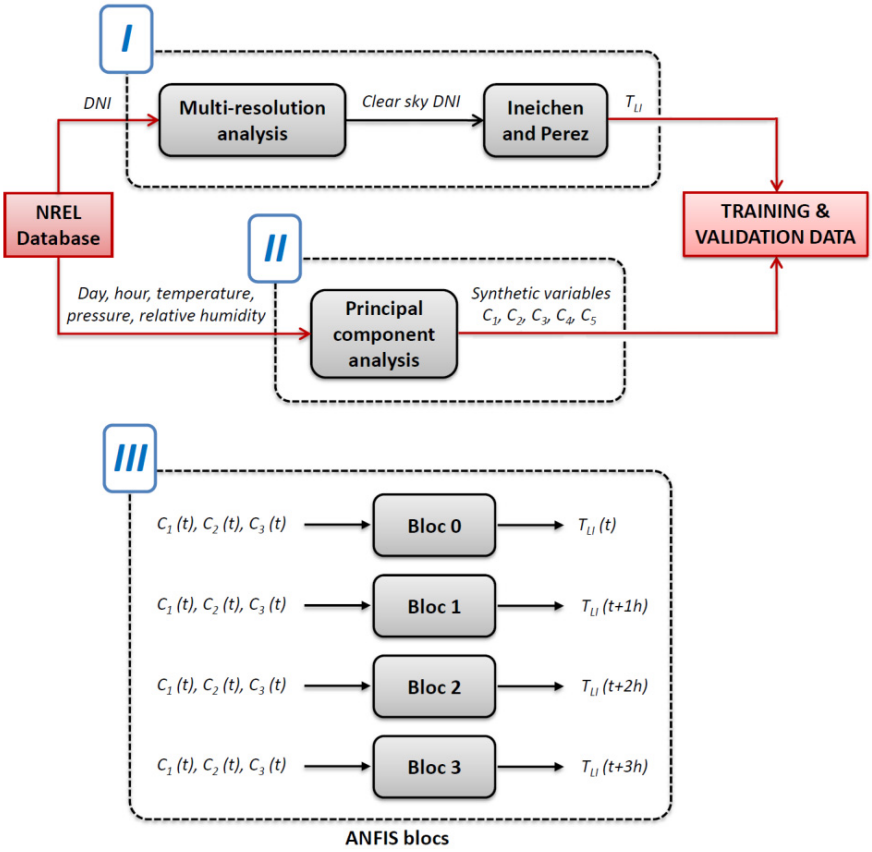

Fig. 1. Diagram of the proposed forecasting approach.

3.3. Wavelet-based multi-resolution analysis

The wavelet-based multi-resolution analysis allows a signal to be decomposed into approximations and details coefficients using a bank of filters composed of Low-Pass (LP) and High-Pass (HP) filters [11]. This process can be repeated *n* times, what produces *n* levels of decomposition, but decomposing (i.e. downsampling) the approximation coefficients (i.e. the low-frequency coefficients) only. The high-frequency coefficients are neglected. Fig.2 shows an example of a multi-resolution analysis. A signal x is first decomposed into an approximation A_1 and a detail D_1 (level 1 of the decomposition). Then, A_1 can be decomposed into an approximation A_2 and a detail D_2 (level 2 of the

decomposition) and so on. Considering n levels of decomposition, the reconstruction process allows the initial signal x to be recovered by simply summing the n details D_1, D_2, ..., D_n and the approximation A_n of level n.

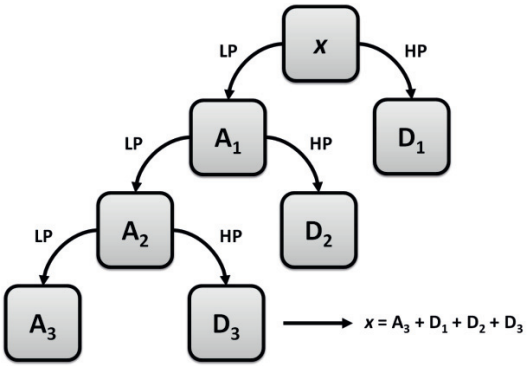

Fig. 2. Multi-resolution analysis leading to the decomposition of level 3 of a given signal x.

Different families of wavelets may be chosen for analyzing sequences of data points. The main criteria are (1) the speed of convergence to 0 of these functions when the time t or the frequency w goes to infinity, which quantifies both time and frequency localizations, (2) the symmetry, (3) the number of vanishing moments of the mother wavelet and (4) the regularity, which is useful for getting nice features, like smoothness of the reconstructed signal. The most commonly used wavelets are the orthogonal ones (Daubechies, Symlet or Coiflet wavelets). Because the Daubechies wavelets [12] have the highest number of vanishing moments, this family has been chosen for carrying out the wavelet-based multi-resolution analysis of the considered sequences of data points.

3.4. Principal component analysis

Principal Component Analysis (PCA) [13,14] uses orthogonal transformation to convert a set of possibly correlated (quantitative) variables x_1, x_2, ..., x_n into a new set of linearly uncorrelated (synthetic) variables y_1, y_2, ..., y_p (with $p \leq n$) called principal components. Basically, PCA allows the principal directions in which the considered data varies to be highlighted. The first component has the largest possible variance and, usually, the first two (or three) components account for most of the variance in the quantitative variables. As a result, PCA is a mathematical procedure allowing the number of variables to be reduced. In other words, it produces a subspace or reasonable dimension so that the projection onto this subspace retains as much from the quantitative information as possible.

Such a procedure is useful in case of a significant number of quantitative variables (n) and if there is some redundancy in those variables. The principal components can be identified by calculating the eigenvectors and the eigenvalues of the covariance matrix, what is equivalent to finding the axis system in which the covariance matrix is diagonal. So, the eigenvector with the largest eigenvalue is the direction of greatest variation, the eigenvector with the second largest eigenvalue is the orthogonal direction with the next highest variation and so on.

3.5. Neuro-fuzzy theory

Fuzzy inference systems (FIS) are also known as fuzzy-rule-based systems [15-19]. Basically, a fuzzy inference system is composed of five functional blocs [20]: (a) a collection of fuzzy if-then rules; (b) a database which defines the membership functions of the fuzzy sets used to design the fuzzy rules; (c) a decision-making unit allowing performing the inference operations on the rules; (d) a fuzzification interface which transforms the crisp inputs into degrees of match with linguistic values; (e) a defuzzification interface which transforms the fuzzy results of the inference into a crisp output. The steps of fuzzy reasoning performed by fuzzy inference systems can be described as follows: (a) the fuzzification step during which the input variables are compared with the membership functions on the premise part to obtain the membership values of each linguistic label; (b) the combination of the membership values on the premise part to get the weight of each rule of the rule base; (c) the generation of the qualified

consequent (fuzzy or crisp) of each rule depending on the weight; (d) the defuzzification step during which the qualified consequents are aggregated to produce a crisp output [21,22].

The acronym ANFIS derives from adaptive network-based fuzzy inference system. A network-type structure, similar to that of artificial neural networks, which maps inputs through input membership functions and associated parameters and then through output membership functions and associated parameters to output, can be used to interpret an input/output map. The parameters associated with the membership functions changes through the learning process. The adjustment of these parameters is facilitated by a gradient vector. This gradient vector provides a measure of how well the fuzzy inference system is modeling the input/output data for a given set of parameters. When the gradient vector is obtained, any of several optimization routines can be applied in order to adjust the parameters to reduce some error measure [23].

For simplicity, we assume, first, that the considered fuzzy inference system has two inputs x and y and one output z and, secondly, that the rule base contains only two fuzzy if-then rules of Takagi and Sugeno's type [19]. The rules are designed in the following way: "*if x is* A_1 *AND y is* B_1 *THEN* $z_1 = p_1x + q_1y + r_1$" (first rule) and "*if x is* A_2 *AND y is* B_2 *THEN* $z_2 = p_2x + q_2y + r_2$" (second rule). Implementing both rules requires a 5-layer ANFIS architecture [24]. A membership function $A_i(x)$ or $B_i(y)$, specifying the degree of which x satisfies A_i or y satisfies B_i, with i = 1,2, is associated with every node in the first layer. Usually $A_i(x)$ and $B_i(y)$ are chosen to be bell-shaped with a minimum and a maximum equal to 0 and 1 respectively (4,5):

$$\mu_{A_i}(x) = \frac{1}{1 + \left(\frac{x - c_i}{a_i}\right)^2 \cdot b_i} \quad \text{or} \quad \mu_{A_i}(x) = exp\left[-\left(\frac{x - c_i}{a_i}\right)^2\right] \tag{4}$$

$$\mu_{B_i}(y) = \frac{1}{1 + \left(\frac{y - c_i'}{a_i'}\right)^2 \cdot b_i'} \quad \text{or} \quad \mu_{B_i}(y) = exp\left[-\left(\frac{y - c_i'}{a_i'}\right)^2\right] \tag{5}$$

with $\{a_i, b_i, c_i\}$and $\{a_i', b_i', c_i'\}$ two parameter sets. As the values of these parameters change, the bell-shaped functions vary accordingly, thus exhibiting various forms of membership functions on linguistic label A_i any continuous and piecewise differentiable functions, such as commonly used trapezoidal or triangular-shaped membership functions, can be used. Nodes in the second layer evaluate the premises of the rules, multiplying the incoming signals and sending the product out [25]. So, the i^{th} node output represents the firing strength of rule i. Let us note that many other T-norm operators, allowing performing generalized AND, can be used in this layer (6):

$$\omega_i = \mu_{A_i}(\mathrm{x}) \times \mu_{B_i}(\mathrm{x}) \quad \text{with } i = 1,2 \tag{6}$$

The i^{th} node in the third layer calculates the ratio of the i^{th} rule's firing strength to the sum of all rules' firing strengths (i.e. the contribution of the i^{th} rule), such as (7):

$$\bar{\omega}_i = \frac{\omega_i}{\omega_1 + \omega_2} \quad \text{with } i = 1,2 \tag{7}$$

Nodes in the fourth layer evaluate the conclusions of the rules. So, the i^{th} node evaluates the conclusion of the i^{th} rule, with $\bar{\omega}_i$ the output of layer 3 and $\{p_i, q_i, r_i\}$ a parameter set. Parameters in this layer can be referred as consequent or conclusion parameters. So (8):

$$\bar{\omega}_i f_i = \bar{\omega}_i(p_i x + q_i y + r_i) \qquad \text{with } i = 1,2 \tag{8}$$

Finally, the single node in the fifth and last layer computes the overall output as the summation of all incoming signals. It is observed that given the values of premise parameters, the overall output can be expressed as a linear combination of the consequent parameters (9):

$$f = \sum_i \bar{\omega}_i f_i = \frac{\sum_i \omega_i f_i}{\sum_i \omega_i} \qquad \text{with } i = 1,2 \tag{9}$$

In order to train an ANFIS, a data set that contains the desired input/output data of the system to be modeled is used. The modeling approach is similar to many system identification techniques: first, you hypothesize a parameterized model structure and next, thanks to an iterative and hybrid optimization method, basically a combination of least squares estimation and backpropagation gradient descent method [26], the membership function parameters are adjusted, the consequent parameters are identified and a rule base is designed, according to a chosen error criterion. The training process stops whenever the maximum iteration number is reached or the training error goal is achieved. In general, this type of modeling works well if the training data presented to the ANFIS is fully representative of the features of the data the trained system is intended to model. Checking and testing data sets allow checking the generalization capability of the resulting fuzzy inference system and avoiding overfitting [27].

4. Results and discussion

4.1. Results of data selection

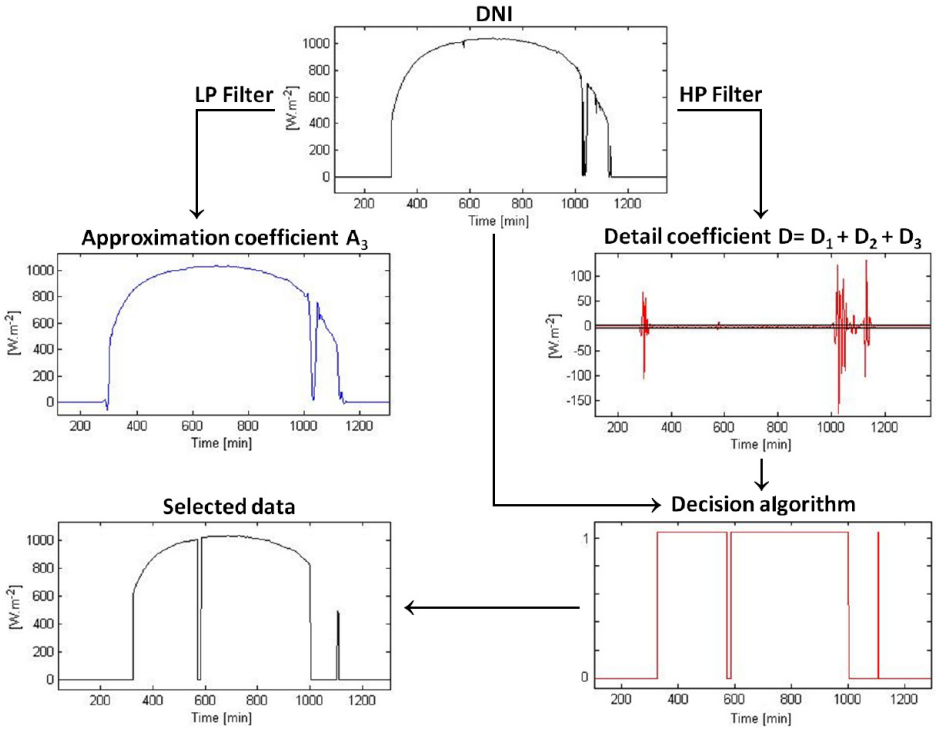

Fig. 3. Clear sky data selection (July 25, 2012).

First, let us note that we used equation (3) to generate historical data about atmospheric turbidity from clear sky DNI values. Such data are needed to develop and validate the atmospheric turbidity forecasting model we propose. So, a decision algorithm has been developed. Such an algorithm allows clear sky data from the NREL database to be extracted and, as a result, data related to significant changes in the DNI to be put aside. First, the wavelet-based multi-resolution analysis we applied to the data allowed the considered daily time series about DNI to be decomposed into n detail coefficients D_1, D_2, ..., D_n. D is the sum of these coefficients. To take a decision, we defined two rules. The first one is formulated as follows: $\forall t$, if $D(t) > 3W.m^{-2}$ (in this case changes in the DNI

are significant and, as a result, the presence of clouds is pretty much sure), $DNI(t)$ is not preserved. The second decision rule allows the low DNI values (during nighttime, at sunshine or sunset) to be removed from the base used to develop and validate the proposed forecasting approach. The second rule is formulated in the following way: $\forall t$, if $DNI(t) < 20W.m^{-2}$, $DNI(t)$ is not preserved. The two considered threshold have been defined empirically.

Table 1. Impact of both the Decomposition Level (DL) and Wavelet Order (WO) on performance (k/a).

DL\WO	1	2	3	4	5
1	C/B	B/B	B/B	B/B	B/B
2	B/C	C/B	C/B	B/B	B/A
3	B/C	C/B	B/B	A/A	A/A
4	B/C	B/B	B/B	A/A	A/A

In order to optimize the proposed algorithm, we carried out a parametric study dealing with choice of the mother wavelet, its order and the decomposition level. We decided for a wavelet from the Daubechies wavelets, a family of orthogonal wavelets characterized by a maximal number of vanishing moments (as a key point, this does not imply the best smoothness). We defined two criteria, denoted k and a, allowing the ability of the proposed algorithm in keeping good samples (i.e. clear sky data) and putting aside bad ones (i.e. covered sky data) to be quantified. Table 1 summarizes the optimization results: "A" is for very good results, "B" is for satisfactory results and "C" is for bad results. Taking a quick look at the above mentioned table, one can highlight the optimal configuration: the best selection of clear sky data is for a Decomposition Level (DL) higher or equal to 3 and a Wavelet Order (WO) higher or equal to 4. As a result, we decided for a decomposition of level 3 and used an order-4 Daubechies wavelet. Fig. 3 shows how the wavelet-based multi-resolution analysis and the proposed decision algorithm allow clear sky data in the NREL database to be selected (July 25, 2012).

4.2. Results of principal component analysis

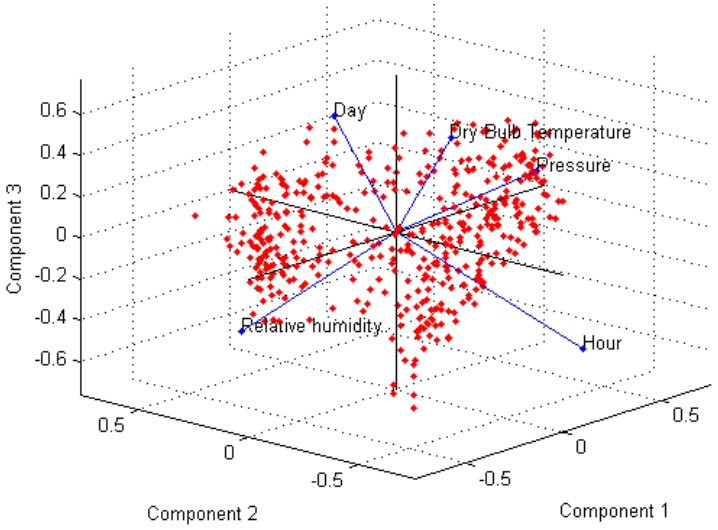

Fig. 4. The first three principal components (C_1, C_2 and C_3) as well as the contribution of day, hour, dry-bulb temperature, and pressure to these components.

Table 2 is about the results of the principal component analysis. Let us remember that we carried out such an analysis in order to generate uncorrelated ANFIS input parameters from day, hour, dry-bulb temperature, relative humidity, and pressure. As previously noted, highly correlated variables impact on learning ability in a negative way. When taking a look at the results we obtained, one can observe that the variance of the first principal component is 60.83%. In addition, the total variance when considering the three first principal components only is

close to 100% (99.68 %). As a result, principal components 4 and 5 do not account for a significant part of this total variance. Finally, we decided for the first three principal components as ANFIS inputs. A reduction in the number of model inputs leads to a reduction in the number of both parameters to be identified and fuzzy rules to be designed during the training phase. As a consequence, the principal component analysis allows both the complexity of the developed model and computation time to be significantly reduced.

Table 2. Principal component analysis (day, hour, dry-bulb temperature, relative humidity, and pressure).

Principal component	C_1	C_2	C_3	C_4	C_5
Variance (%)	60.83	37.86	0.99	0.26	0.06
Total variance (%)	60.83	98.69	99.68	99.94	100

Figure 4 depicts the first three principal components we obtained as well as the contribution of day, hour, dry-bulb temperature, and pressure to these components (99.68% of the total variance). The direction and length of the vectors indicate how each quantitative variable contributes to principal components 1 (C_1), 2 (C_2) and 3 (C_3).

4.3. Forecasting results

Table 3 is about the results we obtained about atmospheric turbidity forecasting (T_{LI}(t), $T_{LI}(t+1h)$, $T_{LI}(t+2h)$ and $T_{LI}(t+3h)$). Let us remember that we considered 84000 examples to develop (56000 examples) and validate (28000 examples) the proposed approach. As a key point, we carried out a parametric study to find the right number of fuzzy sets to be used to split the respective universes of discourse of the three principal components we considered as model inputs. We also tried different membership functions. As a result, we decided for Gaussian membership functions and three fuzzy sets whatever the principal component. After 25 iterations, the hybrid algorithm used during the training phase (basically a combination of least square estimation and backpropagation gradient method) allowed 27 rules (per bloc) to be designed (Table 4). The forecasting results are satisfactory and validate the proposed methodology. The Mean Absolute Error (MAE) is about 0.25 while the Mean Relative Error (MRE) is between 7 and 9%. One can note a slightly increase in both the MAE and MRE with the forecasting horizon, what strongly suggest the robustness of the proposed methodology.

Table 3. Forecasting results (T_{LI}(t), $T_{LI}(t+1h)$, $T_{LI}(t+2h)$ and $T_{LI}(t+3h)$) (validation phase).

Atmospheric turbidity	Mean absolute error (-)	Mean relative error (%)
T_{LI}(t)	0.23	7.57
$T_{LI}(t+1h)$	0.23	7.78
$T_{LI}(t+2h)$	0.26	8.54
$T_{LI}(t+3h)$	0.25	8.35

Table 4. ANFIS model parameters.

Number of training examples	56000
Number of validation examples	28000
Membership functions	Gaussian type
Number of fuzzy sets (per model input)	3
Number of fuzzy rules (per bloc)	27
Number of iterations	25

5. Conclusion and outlook

The CSPIMP (Concentrated Solar Power efficiency IMProvement) European project focuses on optimizing the performance of CSP plants. Because a challenge in the project is to estimate the solar resource, the present work is related to atmospheric turbidity forecasting. First, we used data provided by the NREL (National Renewable Energy Laboratory, Golden, Colorado, USA) to develop and validate an efficient forecasting methodology. Complex

changes in atmospheric turbidity as well as abundant historical data suggest that artificial intelligence techniques are good candidates to forecast atmospheric turbidity accurately from meteorological variables. As a result, side-by-side Adaptive Network-based Fuzzy Inference Systems (ANFIS) have been used. In the field of artificial intelligence, neural networks and fuzzy logic can be combined in neuro-fuzzy systems in order to achieve both properties of readability and learning ability. In addition, a Multi-Resolution Analysis (MRA) based on the discrete wavelet transform allowed DNI values under clear sky conditions (clear sky DNI) to be extracted from the NREL database. We generated historical data about atmospheric turbidity using the empirical formulation proposed by Ineichen and Perez. A Principal Component Analysis (PCA) has been also considered in order to develop the forecasting model using uncorrelated input variables. In addition, PCA allows both the complexity of the developed model and computation time to be significantly reduced. The considered side-by-side ANFIS allow atmospheric turbidity to be forecasted at different time horizons ranging from 1 hour to 3 hours. The forecasting results are satisfactory and validate the proposed methodology. Over 28000 validation examples, the Mean Absolute Error (MAE) is about 0.25 while the Mean Relative Error (MRE) is between 7 and 9%. One can note a slightly increase in both the MAE and MRE with the forecasting horizon, what strongly suggest the robustness of the proposed methodology. In the next months, the proposed methodology will contribute to the development of an advanced control scheme based on a MPC controller for CSP plants. MPC is commonly used to control industrial processes in real time and has good properties of stability and robustness.

References

[1] Ricardo Marquez and Carlos F.M. Coimbra. Forecasting of global and direct solar irradiance using stochastic learning methods, ground experiments and the {NWS} database. *Solar Energy*, 85(5):746 – 756, 2011.

[2] Ricardo Marquez and Carlos F.M. Coimbra. Intra-hour {DNI} forecasting based on cloud tracking image analysis. *Solar Energy*, 91(0):327 – 336, 2013.

[3] C.S.G. Lee C.T. Lin. Neural fuzzy systems: A neuro-fuzzy synergism to intelligent systems. *Prentice Hall, Upper Saddle River, NJ*, 1996.

[4] A. Abraham. Adaptation of fuzzy inference system using neural learning. *fuzzy system engineering: theory and practice, in: N. Nedjah, et al. (Eds.), Studies in Fuzziness and Soft Computing, Springer Verlag, Germany.*, vol. 3:pp. 53–83., 2005.

[5] WE Alnaser and NS Awadalla. The linke turbidity factor and ångström coefficient in humid climate of bahrain. *Earth, Moon, and Planets*, 70(1-3):61–74, 1995.

[6] Linke F. Transmisions-koeffizient und trübungsfaktor. *Beitr. Physik. fr. Atmos.*, 10:91–103, 1922.

[7] F Kasten. Elimination of the virtual diurnal variation of the linke turbidity factor. *Meteorologische Rundschau*, 41(3):93–94, 1988.

[8] JC Grenier, A de La Casinière, and T Cabot. A spectral model of linke's turbidity factor and its experimental implications. *Solar Energy*, 52(4):303–313, 1994.

[9] Fritz Kasten and Andrew T Young. Revised optical air mass tables and approximation formula. *Appl. Opt*, 28(22):4735–4738, 1989.

[10] Pierre Ineichen and Richard Perez. A new airmass independent formulation for the linke turbidity coefficient. *Solar Energy*, 73(3):151 – 157, 2002.

[11] Stéphane Mallat. *A wavelet tour of signal processing*. Access Online via Elsevier, 1999.

[12] Ingrid Daubechies et al. *Ten lectures on wavelets*, volume 61. SIAM, 1992.

[13] Jonathon Shlens. A tutorial on principal component analysis. *Systems Neurobiology Laboratory, University of California at San Diego*, 2005.

[14] Achmad Muslim, Toni Bakhtiar, et al. Variable selection using principal component and procrustes analyses and its application in educational data. *Journal of Asian Scientific Research*, 2(12):856–865, 2012.

[15] Y. Hayashi J.J. Buckley. Fuzzy neural networks: a survey. *Fuzzy Sets and Systems*, 66:1–13, 1994.

[16] Y. Hayashi J.J. Buckley. Neural networks for fuzzy systems. *Fuzzy Sets and Systems*, 7:265–276., 1995.

[17] L. Zadeh. Fuzzy sets. *Information and Control*, 8:338–353, 1965.

[18] L. Zadeh. Outline of a new approach to the analysis of complex systems and decision processes. *IEEE Transactions on Systems, Man, and Cybernetics*, 3:28–44, 1973.

[19] M. Sugeno T. Takagi. Derivation of fuzzy control rules from human operator's control actions. *in: Proc. IFAC Symp. Fuzzy Inform., Knowledge Representation and Decision Analysis*, page 55–60, 1983.

[20] J.S.R. Jang. Anfis: adaptative-network-based fuzzy inference system. *IEEE Transactions on Systems, Man, and Cybernetics*, 23 (3):665–685, 1993.

[21] C.C. Lee. Fuzzy logic in control systems: fuzzy logic controller - part i. *IEEE Transactions on Systems, Man, and Cybernetics*, 20:404–418, 1990.

[22] C.C. Lee. Fuzzy logic in control systems: fuzzy logic controller - part ii. *IEEE Transactions on Systems, Man, and Cybernetics*, 20:419–435, 1990.

[23] C.T. Sun J.S.R. Jang. Neuro-fuzzy modeling and control. *IEEE Proceedings*, 83 (3):378–406, 1995.

[24] H. White K. Hornik, M. Stinchcombe. Multi-layer feedforward networks are universal approximation. *Neural Networks*, 2:359–366, 1989.

[25] E. Pap E.P. Klement, R. Mesiar. Triangular norms. *Kluwer Academics Publishers, Dordrecht, The Netherlands*, 2000.
[26] C. Charalambous. Conjugate gradient algorithm for efficient training of artificial neural networks. *IEEE Proceedings*, 139:301–310, 1992.
[27] W. Brauer C. Schittenkopf, G. Deco. Two strategies to avoid overfitting in feedforward networks. *Neural Networks*, 10:505–516, 1997.